Predicting sites of new hemorrhage with amyloid imaging in cerebral amyloid angiopathy

M. Edip Gurol, MD
Gregory Dierksen, MEng
Rebecca Betensky, PhD
Christopher Gidicsin, BA
Amy Halpin, BA
Alex Becker, PhD
Jeremy Carmasin, BA
Alison Ayres, BA
Kristin Schwab, BA
Anand Viswanathan, MD, PhD
David Salat, PhD
Jonathan Rosand, MD, MSc
Keith A. Johnson, MD
Steven M. Greenberg, MD, PhD

Correspondence & reprint requests to Dr. Gurol: egurol@yahoo.com

ABSTRACT

Objective: We aimed to determine whether amyloid imaging can help predict the location and number of future hemorrhages in cerebral amyloid angiopathy (CAA).

Methods: We performed a longitudinal cohort study of 11 patients with CAA without dementia who underwent serial brain MRIs after baseline amyloid imaging with Pittsburgh compound B (PiB). Mean distribution volume ratio (DVR) of PiB was determined at the sites of new micro/macrobleeds identified on follow-up MRI and compared with PiB retention at "simulated" hemorrhages, randomly placed in the same subjects using a probability distribution map of CAA-hemorrhage location. Mean PiB retention at the sites of observed new bleeds was also compared to that in shells concentrically surrounding the bleeds. Finally the association between number of incident bleeds and 3 regional amyloid measures were obtained.

Results: Nine of 11 subjects had at least one new microbleed on follow-up MRI (median 4, interquartile range [IQR] 1–9) and 2 had 5 new intracerebral hemorrhages. Mean DVR was greater at the sites of incident bleeds (1.34, 95% confidence interval [CI] 1.23–1.46) than simulated lesions (1.14, 95% CI 1.07–1.22, $p < 0.0001$) in multivariable models. PiB retention decreased with increasing distance from sites of observed bleeds ($p < 0.0001$). Mean DVR in a superior frontal/parasagittal region of interest correlated independently with number of future hemorrhages after adjustment for relevant covariates ($p = 0.003$).

Conclusions: Our results provide direct evidence that new CAA-related hemorrhages occur preferentially at sites of increased amyloid deposition and suggest that PiB-PET imaging may be a useful tool in prediction of incident hemorrhages in patients with CAA. *Neurology*® 2012;79:320–326

GLOSSARY

Aβ = β-amyloid; **CAA** = cerebral amyloid angiopathy; **CI** = confidence interval; **DVR** = distribution volume ratio; **IQR** = interquartile range; **PiB** = Pittsburgh compound B; **ROI** = region of interest; **SWI** = susceptibility-weighted imaging.

Small vessel brain disease is associated with a range of brain lesions including white matter T2 hyperintensities, cerebral microbleeds, lacunar lesions, and cerebral microinfarcts.[1–3] The precise relationship between location of the small vessel pathology and the resultant brain lesions has been difficult to establish, however, largely because of inability to image the small vessels during life. An important advance in this regard was the development of the thioflavin T derivative Pittsburgh compound B (PiB) for in vivo imaging of fibrillar β-amyloid (Aβ). A series of studies have demonstrated that PiB labels not only parenchymal Aβ in senile plaques[4] but also the cerebrovascular Aβ deposits[5–9] that define cerebral amyloid angiopathy (CAA).

A spatial relationship between vascular amyloid and lobar bleeds in CAA has been suggested by neuropathologic studies[10,11] and one cross-sectional radiologic analysis using PiB-PET imaging.[12] There are no prospective studies of patients with CAA followed over time, however, making it difficult to determine the cause-effect relationship between amyloid deposits and bleeding or whether amyloid burden continues to predict bleeding in patients with CAA after their initial presentation and diagnosis. We therefore performed a longitudinal study to address

From the Departments of Neurology (M.E.G., G.D., A.H., A.A., K.S., A.V., J.R., S.M.G.) and Radiology (C.G., A.B., J.C., D.S., K.A.J.), Massachusetts General Hospital, Boston; and the Department of Biostatistics (M.E.G., R.B.), Harvard School of Public Health, Boston, MA.
Study funding: Supported by NIH (T32NS048005, 5R01NS070834-01/02, R01AG026484).
Go to Neurology.org for full disclosures. Disclosures deemed relevant by the authors, if any, are provided at the end of this article.

whether PiB-PET imaging can predict sites of impending hemorrhage, and more broadly, whether overall PiB burden provides information about the likelihood of future bleeding throughout the brain.

METHODS

Study subjects. We performed a prospective, longitudinal cohort study of 11 patients with CAA who underwent baseline PiB-PET and MRI (including T2*-weighted sequences) followed by a second follow-up MRI at least 12 months later. The subjects were recruited from an ongoing single-center prospective longitudinal cohort study of the natural history of CAA.[13] Detailed information including demographics, clinical status, risk factors, and characteristics of the presenting event were prospectively recorded at the time of cohort entry. None of the 11 subjects had dementia and all were free of symptoms suggestive of new stroke for 1 year prior to PiB-PET. None of the patients were treated with anticoagulation. All 11 subjects met criteria for probable CAA according to Boston criteria,[14] including supporting CAA pathology in 4 subjects. The *APOE* genotype was determined from patients' blood samples as previously described.[15]

Standard protocol approvals, registrations, and patient consents. This study was performed with the approval of and in accordance with the guidelines of the institutional review board of Massachusetts General Hospital and with the informed consent of all subjects or family members.

Imaging acquisition and analysis. All subjects had a PiB-PET scan between April 2006 and January 2009 as previously described.[7] In brief, N-methyl-[^{11}C]2-(4-methylaminophenyl)-6-hydroxybenzothiazole (PiB) was prepared at Massachusetts General Hospital. Subjects were positioned in either of 2 PET cameras for dynamic acquisition, a Siemens/CTI ECAT HR+ scanner (3D mode; 63 image planes; 15.2 cm axial field of view; 5.6 mm transaxial resolution and 2.4 mm slice interval; 69 frames: 12 × 15 seconds, 57 × 60 seconds, Knoxville, TN) or a GE PC4096 scanner (2D mode; 15 image planes; 10.0 cm axial field of view; 7.0 mm transaxial resolution and 6.0 mm slice interval; 39 frames: 8 × 15 seconds, 4 × 60 seconds, 27 × 120 seconds, Milwaukee, WI). After a transmission scan, 8.5 to 15 mCi ^{11}C-PiB was injected as a bolus and followed immediately by a 60-minute dynamic acquisition. Distribution volume ratio (DVR) was calculated for each voxel using cerebellar cortex as the reference tissue input function and whole brain parametric images were constructed. DVR in 3 predefined regions of interest (ROI) routinely used in our PET laboratory were calculated for each subject as an overall measure of PiB retention: mean global, mean superior frontal/parasagittal, and mean occipital DVR values.[7] Each of these aggregate ROIs included the full thickness of the cortex and immediate subcortical white matter in these regions. Anatomic descriptions of the global and occipital ROIs have been previously reported.[7] The superior frontal/parasagittal ROI included bilateral superior and middle frontal gyri (both medial and lateral aspects) and precuneus.[16]

Each patient underwent research T2*-weighted MRI for detection of cerebral hemorrhages within 1 month after PiB-PET imaging and a further follow-up T2*-weighted MRI to identify new (incident) bleeds at least 12 months later. Previously described protocols were used to obtain gradient-echo or susceptibility-weighted imaging (SWI) MRI scans at 1.5 T.[17] Each subject had the baseline and follow-up scans performed using the same imaging protocol and scanner. Microbleeds were identified according to previously published guidelines.[18] An experienced rater blinded to the results of the PiB-PET scans reviewed the 2 MRI scans and manually traced incident microbleeds and macrobleeds (figure 1, A–C) using the Freeview tool incorporated into Freesurfer image analysis suite (documented and freely available at http://surfer.nmr.mgh.harvard.edu/). The number and location of hemorrhagic lesions at baseline and new microbleeds at follow-up were recorded for each patient. The incident hemorrhage ROIs were saved as a 3D map for each patient. To generate an appropriate comparison for the incident bleeds, a previously validated computer script placed 200 "simulated" bleeds on the second T2* MRIs according to a centroid probability distribution function derived from 370 hemorrhagic lesions detected by T2*-weighted MRI of 51 subjects with probable CAA.[12] These "simulated" bleed maps were visually inspected to correct for overlap with actual bleeds as well as regions outside of brain parenchyma; any such occurrence was deleted and the resultant control maps were saved. Another previously described computer script was used to obtain 5 concentric ROIs (shells) of 2 mm thickness each, around the actual and simulated lesions.[12]

The PiB-PET scans were coregistered to the second T2* MRI scans containing the observed incident and simulated control bleed maps using the tkregister tool in the Freesurfer Image

Figure 1 Methods for image analysis

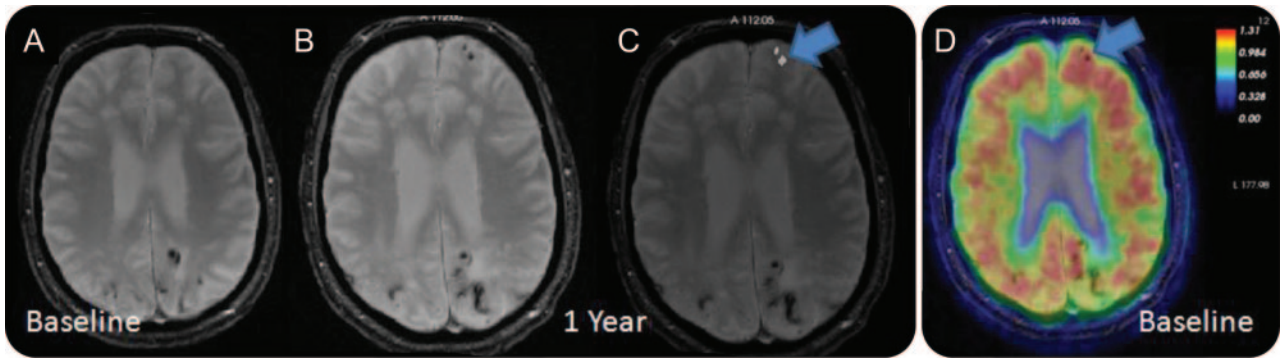

Baseline (A) and follow-up (B) T2* MRIs are reviewed by a rater blinded to the Pittsburgh compound B (PiB) PET scans, new bleeds are identified and mapped on the follow-up MRI (arrow, C). At the last step, follow-up T2* MRI and PiB-PET scans are coregistered for every patient and mean distribution volume ratio values are calculated for each bleed from the corresponding areas on PET (arrow, D).

Analysis suite. Mean DVR values corresponding to the locations of each incident or simulated hemorrhage were obtained from the PiB-PET scans (figure 1D). Mean DVR values corresponding to the 5 concentric ROIs surrounding the actual and control bleeds were similarly obtained.

Statistical analysis. Bivariate comparisons were performed using χ^2 test for ratios and *t* test or Wilcoxon rank sum test for continuous variables depending on their distribution. Mean PiB-PET DVR values were compared between 1) sites of observed incident bleeds and sites of simulated bleeds, and 2) sites of incident bleeds and the 5 concentric shells placed at increasing distances around them. These primary analyses were performed by linear mixed-effects models to account for fixed effects (age, gender, number of bleeds at first MRI, time between PiB-PET and second MRI, number of new microbleeds) and random effects (controlling for subject-specific contributions). We also calculated the bivariate associations between the number of new bleeds on follow-up MRI scan and potential predictors including mean aggregate DVR values from 3 prespecified aggregated ROIs on PiB PET, number of baseline microbleeds, age, and *APOE* genotype. Multivariate linear regression analysis was then used to identify independent predictors of number of incident bleeds. Covariates for all multivariable models were identified based on the results of bivariate analyses in this study and findings from previous reports.[15,18–20] Linear mixed-effects models were built using SAS software; all other statistical analyses were performed using Stata software. A threshold for significance of $p < 0.05$ was used, with the exception of a Bonferroni-corrected threshold of $p < 0.017$ applied to analyses of the 3 aggregate ROIs. All tests of significance were 2-tailed.

RESULTS Characteristics of the study group. Demographic and imaging characteristics of the 11 subjects with CAA are presented in the table; 9 of the 11 were male. They presented with symptomatic intracerebral hemorrhage (n = 5) or with other symptoms (n = 6) such as seizures or gait problems. None had cognitive symptoms that interfered with daily functioning. As shown in the table, 9 of the subjects had new microbleeds (median of 4 new lesions) over an average 19-month follow up. Two of these 9 patients had a total of 5 new macrohemorrhages on follow-up. There was no difference between probable CAA patients with vs without supporting pathology in incident bleed counts ($p = 0.4$) or in global, frontal, and occipital PiB retention (all $p > 0.9$). Mean global, occipital, and superior frontal/parasagittal DVRs were not different between these 11 subjects and 18 other patients with CAA who underwent PiB-PET but did not meet eligibility criteria for the current analysis ($p > 0.2$ for all comparisons). Similarly, comparison of the lobar distribution of hemorrhages in the current study with a separate cohort of 51 patients with CAA with a total of 321 hemorrhages[21] showed no difference in the distribution of baseline, incident, or all hemorrhages ($p > 0.2$ for all comparisons), suggesting that the current study group is representative of our overall CAA research population.

Table Characteristics of the patient cohort[a]

	Patients	Total no.	Mean (SD) or median (IQR)
Age	11		70.9 (8.6)
MMSE	11		29 (28–30)
Months from PET to follow-up MRI	11		19 (14–33)
Initial MB count	11	381	14 (2–42)
New MB	9	68	4 (1–9)
New ICH	2	5	

Abbreviations: ICH = intracerebral hemorrhage; IQR = interquartile range; MB = microbleed; MMSE = Mini-Mental State Examination.
[a] Median values are presented, with the exception of mean age.

Comparison of amyloid deposition between sites of actual incident hemorrhages vs control simulated hemorrhages. We analyzed whether higher PiB retention at baseline identified sites of future hemorrhage. Using linear mixed-effects models to account for age, gender, number of hemorrhages at first MRI, time between PiB-PET and second MRI, number of new microbleeds, and subject-specific contributions, mean DVR was greater ($p < 0.0001$) within the sites of the incident observed hemorrhages (mean = 1.34, 95% confidence interval [CI] 1.23–1.46) than simulated hemorrhages placed according to a probability density map (mean = 1.14, 95% CI 1.07–1.22). None of the other fixed effects mentioned above was significant in this model. Increased PiB retention appeared to characterize sites of future macrobleeds as well as microbleeds (figure 2), though the few incident macrobleeds precluded a separate analysis. Very similar results were obtained when the new macrohemorrhages were excluded and the analysis was restricted to microbleeds (mean DVR = 1.34, 95% CI 1.22–1.45 for observed CMB; 1.14 and 1.07, 1.22 for simulated CMB, $p < 0.0001$). The baseline amyloid load did not differ between sites of incident microbleeds and macrohemorrhages ($p = 0.13$). Using a cutpoint DVR of 1.22 (the lower limit of the CI for actual new microbleeds and the upper limit for the simulated microbleeds), we found that lobar locations with elevated PiB retention had increased risk of having an incident bleed (odds ratio = 5.21, 95% CI 3.06–8.88, $p < 0.0001$).

We also analyzed the falloff of DVR between the center of the observed bleeds and each of 5 surrounding 2-mm-thick ROIs. Mean DVR decreased with increasing distance from the center for observed new bleeds ($p < 0.0001$) by an average of 0.034 ± 0.003 per shell. Despite the decrease in DVR with increasing distance from the centers of the observed hemorrhages, the values in each of these concentric shells were greater than the corresponding shells placed around the sites of simulated hemorrhages (figure 3).

Figure 2 Appearance of an intracerebral hemorrhage at a location with baseline high amyloid deposition

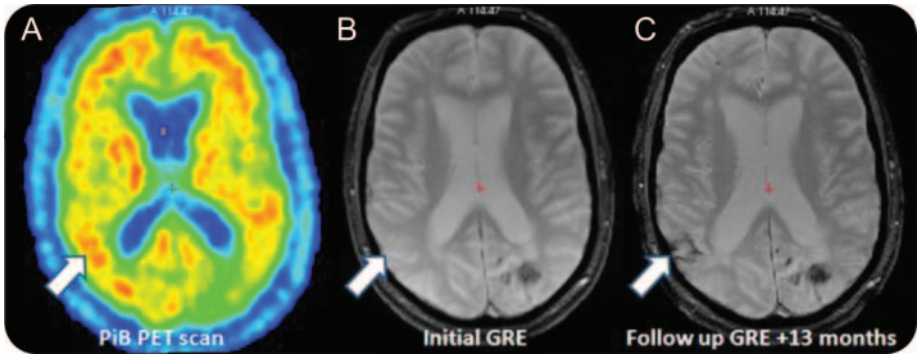

Arrows point to an area with high Pittsburgh compound B (PiB) retention on baseline PET (A), without hemorrhage on initial T2* MRI scan (B), and where a hemorrhage appears on the 13-month follow-up T2* MRI (C). GRE = gradient echo.

Mean PiB PET values in prediction of incident hemorrhages. We tested 3 prespecified measures of overall baseline PiB retention as potential predictors of future risk of hemorrhage at any site. Mean DVR of an aggregate superior frontal/parasagittal ROI that includes bilateral middle and superior frontal gyri and precuneus showed a strong correlation with the number of incident microbleeds on follow-up MRI ($\rho = 0.76$, $p = 0.007$) in this small sample (figure 4), significant at the Bonferroni-corrected threshold used to account for the 3 ROIs tested. The association between PiB retention in this ROI and number of incident microbleeds remained independent ($p = 0.003$) after adjustment for number of baseline microbleeds, age, and *APOE* genotype. This association did not change when the total number of incident hemorrhagic lesions (microbleeds + macrobleeds) was used as the outcome measure, instead of new microbleed counts. The number of microbleeds at baseline was the only other independent predictor of incident microbleeds on follow-up ($p = 0.001$). Incident microbleeds were not predicted by mean DVR in the other 2 examined ROIs: aggregated global ($\rho = 0.47$, $p = 0.14$) and occipital ($\rho = 0.21$, $p = 0.5$) regions.

Figure 3 Linear falloff of distribution volume ratio (DVR) values around incident microbleeds

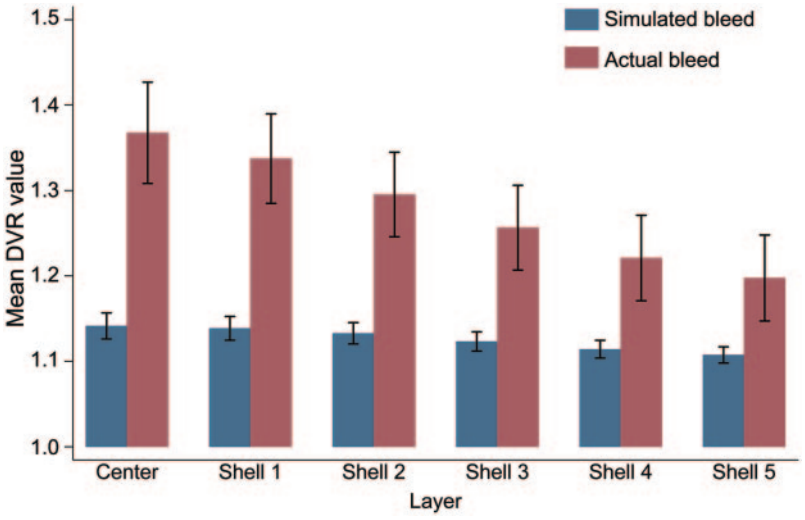

Amyloid deposition decreases at increasing distances from the sites of incident bleeds. The centers and immediate peripheries of actual bleeds have higher Pittsburgh compound B retention when compared to the corresponding shells in and around simulated bleeds.

DISCUSSION The major finding from this analysis was that new hemorrhagic lesions in patients with CAA occur preferentially at sites in which PiB retention was elevated at baseline. PiB retention at sites of future bleeding was significantly greater than other locations typical of CAA-related hemorrhage (identified by a probability density map compiled across other CAA subjects) and higher than regions at increasing distances from the site of incident hemorrhage. The difference in multivariable-adjusted mean DVR at observed vs simulated hemorrhage sites (1.34 vs 1.14) represents a 2.4-fold increase above the expected background DVR of 1, and thus appears to represent a substantial elevation in local amyloid deposition. We additionally found that overall burden of CAA in a superior frontal/parasagittal ROI was an independent predictor for number of future hemorrhages, a further indication of the link between vascular amyloid burden and risk of bleeding.

The longitudinal results strongly support the idea that local accumulations of amyloid trigger future vessel rupture and hemorrhage. The association between sites of hemorrhage and PiB seen in prior cross-sectional analysis[12] did not identify which finding preceded the other, leaving open the possibility that local blood might somehow promote PiB retention rather than vice versa. Histopathologic staining did not find that hemorrhage products bind PiB, however,[12] and the current longitudinal analysis fully establishes that elevations of PiB precede the

Figure 4 Correlation between mean superior frontal/parasagittal distribution volume ratio (DVR) and incident microbleed counts

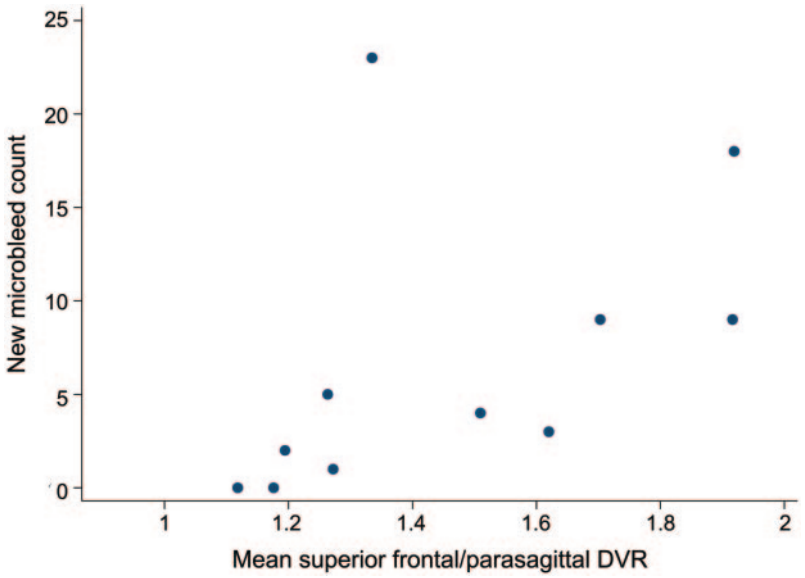

The number of new microbleeds correlated with mean DVR in a superior frontal/parasagittal region of interest ($\rho = 0.76$, $p = 0.007$).

occurrence of bleeding. Another idea supported by the current findings is that sites of higher amyloid burden continue to mark increased risk of further bleeding in individuals after their initial clinical presentation, when they could potentially be treated with (as yet unidentified) disease-modifying therapies.

We observed that PiB retention in the superior frontal/parasagittal region predicted number of future hemorrhages, independent of other known predictors such as baseline hemorrhage count, and significant after correction for multiple hypothesis testing. If this finding is confirmed, PiB PET might offer the potential for detecting patients with CAA at increased risk of incident hemorrhages at a relatively early stage of their disease. CAA shows a general predilection for posterior brain regions[22] and the distribution of PiB in advanced CAA is characterized by relatively greater occipital signal compared to patients with AD.[7,9] We nonetheless observed that among patients with CAA without dementia, those with highest upper convexity burdens tended to have more new hemorrhages at follow-up (figure 4). This result was unexpected and clearly requires replication. If confirmed, a possible explanation is that while CAA tends to produce relatively high occipital burdens, greater disease severity among patients with CAA may actually correlate with increasing deposition in upper convexity. It is also possible that CAA's occipital predilection could affect PiB retention via flow-related mechanisms, such that occipital retention may not as closely reflect underlying amyloid pathology as frontal and precuneus PiB. To help exclude the further possibility that this small group was not representative of patients with CAA at large, we compared the distribution of baseline and incident hemorrhages in our cohort with the microbleed distribution in a previously published larger cohort of patients with CAA[21] and found no differences. This result suggests that our patient group was not substantially different from other patients diagnosed with CAA.

This longitudinal analysis of PiB retention and hemorrhage location suffers from several methodologic limitations. One limitation is the small sample size (11 subjects, 73 new hemorrhage lesions), which was nonetheless sufficient to yield strong statistical associations. We also note that PET imaging has relatively poor spatial resolution, causing some imprecision in our ability to colocalize PiB retention and hemorrhage location. Importantly, both of these sources of error would be expected to bias the data toward the null hypothesis (that there is no relationship between the 2 lesions) rather than toward a positive association. Another factor to consider in our analysis is the role of parenchymal Alzheimer pathology, as senile plaques,[4] like vascular amyloid,[5–7,9] bind PiB. Amyloid-containing parenchymal plaques and vascular amyloid pathology often coexist in AD and CAA.[8] It is therefore likely that at least part of the PiB retention in our cohort resulted from parenchymal (rather than vascular) amyloid pathology, which may contribute as a risk indicator for incident hemorrhage. There are nevertheless several arguments indicating that vascular amyloid is mechanistically responsible for incident hemorrhages in this CAA cohort. There are no established mechanisms by which parenchymal amyloid deposits cause hemorrhage, suggesting that the observed spatial associations between amyloid burden and incident hemorrhages reflect CAA rather than AD pathology. Also, our patient cohort had normal Mini-Mental State Examination scores (median 29, IQR 28–30) and none had dementia clinically, arguing against the presence of full-blown AD pathology. Thus although some degree of overlap in parenchymal and vascular amyloid deposits is inevitable in both CAA and AD research, the observed data are suggestive of a robust underlying spatial association between CAA severity and incident hemorrhage.

One implication of the current results is to offer further support for the possibility that preventing or reducing vascular amyloid might lower the risk of future CAA-related bleeding. This possibility has not yet been directly tested, and indeed animal and human studies of anti-amyloid immunotherapy have suggested a complex picture in which bleeding risk may be increased at least transiently.[23,24] Another

possibility raised by these data are that markers of overall amyloid burden, such as the composite superior frontal/parasagittal ROI identified in the current study, may find clinical use as predictors of hemorrhage risk. Determining hemorrhage risk plays an important role in clinical decision-making, particularly for determining when the benefits of long-term anticoagulation outweigh its risk.[25] Although it is unclear whether amyloid imaging will offer strong enough prognostic information to tip clinical decisions toward or away from anticoagulation, this approach represents an intriguing potential tool for risk stratification in patients with CAA.

AUTHOR CONTRIBUTIONS

M.E. Gurol: study concept/design, contribution of vital reagents/tools/patents, study supervision/coordination, acquisition of data, statistical analysis/interpretation of data, drafting/revising the manuscript for content. G. Dierksen: study concept/design, contribution of vital reagents/tools/patents, study supervision/coordination, acquisition of data. R. Betensky: study concept/design, statistical analysis/interpretation of data, contribution of vital reagents/tools/patents, obtaining funding. C. Gidicsin: study coordination, acquisition of data, contribution of vital reagents/tools/patents. A. Halpin: study coordination, acquisition of data, contribution of vital reagents/tools/patents. A. Becker: study coordination, acquisition of data, contribution of vital reagents/tools/patents. J. Carmasin: study coordination, acquisition of data, contribution of vital reagents/tools/patents. A. Ayres: study supervision/coordination, acquisition of data, contribution of vital reagents/tools/patents. K. Schwab: study supervision/coordination, acquisition of data, obtaining funding. A. Viswanathan: study supervision/coordination, contribution of vital reagents/tools/patents, drafting/revising the manuscript for content. D. Salat: study concept/design, contribution of vital reagents/tools/patents. J. Rosand: study concept/design, study supervision/coordination, drafting/revising the manuscript for content. K.A. Johnson: study concept/design, contribution of vital reagents/tools/patents, acquisition of data, drafting/revising the manuscript for content. S.M. Greenberg: study concept/design, study supervision/coordination, contribution of vital reagents/tools/patents, interpretation of data, drafting/revising the manuscript for content, obtaining funding.

DISCLOSURE

M.E. Gurol receives research support from the NIH (T32NS048005, R01 NS070834-02). G. Dierksen reports no disclosures. R. Betensky has received funding from NIH for the development of statistical methodology and for collaborations in brain tumors, stroke, CAA, Alzheimer disease, cancer, and multiple sclerosis. She has received funding from the Harvard NeuroDiscovery Center and the Harvard Catalyst (CTSA) for statistical support of collaborative projects. She has received funding from Bristol Myers Squibb and NIH for DSMB service, from Novartis for statistical methodology development with applications to MS, and from Maine Medical Center, Arex, Sekisui, Gerson Lehrman Group, Leerink Swann, Guidepoint Global, HLM Venture Partners, Clinical Trials Solutions, and Cowen Inc. for general statistical consultation. C. Gidicsin, A. Halpin, A. Becker, J. Carmasin, A. Ayres, K. Schwab, A. Viswanathan, D. Salat, J. Rosand, and K.A. Johnson report no disclosures. S.M. Greenberg served on Scientific Advisory Boards (1-NINDS Data Safety Monitoring Board for clinical trials in intracerebral hemorrhage, 2-Hoffman-Laroche, MRI Review Committee) and has received funding for travel or speaker honoraria (Medtronics, research lecture, 2010 Pfizer Global Research and Development, research lecture, 2010). Dr. Greenberg is also on the editorial boards of several journals (*Stroke*, Editorial Board, 2010–present; *Cerebrovascular Disease*, Editorial Board, 2008–present; *Neurology*®, Editorial Board, 2005–present; *Journal of Alzheimer's Disease and Other Dementias*, Editorial Board, 2005–present). Dr. Greenberg worked as a consultant for Hoffman-LaRoche, Janssen Alzheimer Immunotherapy, and Bristol-Myers Squibb Company. He received research support from the NIH. **Go to Neurology.org for full disclosures.**

Received November 3, 2011. Accepted in final form March 19, 2012.

REFERENCES

1. Gouw AA, Seewann A, van der Flier WM, et al. Heterogeneity of small vessel disease: a systematic review of MRI and histopathology correlations. J Neurol Neurosurg Psychiatry 2011;82:126–135.
2. Pantoni L. Cerebral small vessel disease: from pathogenesis and clinical characteristics to therapeutic challenges. Lancet Neurol 2010;9:689–701.
3. van Es AC, van der Grond J, de Craen AJ, et al. Cerebral microbleeds and cognitive functioning in the PROSPER study. Neurology 2011;77:1446–1452.
4. Klunk WE, Engler H, Nordberg A, et al. Imaging brain amyloid in Alzheimer's disease with Pittsburgh compound-B. Ann Neurol 2004;55:306–319.
5. Bacskai BJ, Frosch MP, Freeman SH, et al. Molecular imaging with Pittsburgh compound B confirmed at autopsy: a case report. Arch Neurol 2007;64:431–434.
6. Greenberg SM, Grabowski T, Gurol ME, et al. Detection of isolated cerebrovascular beta-amyloid with Pittsburgh compound B. Ann Neurol 2008;64:587–591.
7. Johnson KA, Gregas M, Becker JA, et al. Imaging of amyloid burden and distribution in cerebral amyloid angiopathy. Ann Neurol 2007;62:229–234.
8. Lockhart A, Lamb JR, Osredkar T, et al. PIB is a non-specific imaging marker of amyloid-beta (Abeta) peptide-related cerebral amyloidosis. Brain 2007;130:2607–2615.
9. Ly JV, Donnan GA, Villemagne VL, et al. ^{11}C-PIB binding is increased in patients with cerebral amyloid angiopathy-related hemorrhage. Neurology 2010;74:487–493.
10. Maeda A, Yamada M, Itoh Y, Otomo E, Hayakawa M, Miyatake T. Computer-assisted three-dimensional image analysis of cerebral amyloid angiopathy. Stroke 1993;24:1857–1864.
11. Vonsattel JP, Myers RH, Hedley-Whyte ET, Ropper AH, Bird ED, Richardson EP Jr. Cerebral amyloid angiopathy without and with cerebral hemorrhages: a comparative histological study. Ann Neurol 1991;30:637–649.
12. Dierksen GA, Skehan ME, Khan MA, et al. Spatial relation between microbleeds and amyloid deposits in amyloid angiopathy. Ann Neurol 2010;68:545–548.
13. Smith EE, Gurol ME, Eng JA, et al. White matter lesions, cognition, and recurrent hemorrhage in lobar intracerebral hemorrhage. Neurology 2004;63:1606–1612.
14. Knudsen KA, Rosand J, Karluk D, Greenberg SM. Clinical diagnosis of cerebral amyloid angiopathy: validation of the Boston criteria. Neurology 2001;56:537–539.
15. O'Donnell HC, Rosand J, Knudsen KA, et al. Apolipoprotein E genotype and the risk of recurrent lobar intracerebral hemorrhage. N Engl J Med 2000;342:240–245.
16. Tzourio-Mazoyer N, Landeau B, Papathanassiou D, et al. Automated anatomical labeling of activations in SPM using a macroscopic anatomical parcellation of the MNI MRI single-subject brain. NeuroImage 2002;15:273–289.
17. Gurol ME, Irizarry MC, Smith EE, et al. Plasma beta-amyloid and white matter lesions in AD, MCI, and cerebral amyloid angiopathy Neurology 2006;66:23–29.

18. Greenberg SM, Vernooij MW, Cordonnier C, et al. Cerebral microbleeds: a guide to detection and interpretation. Lancet Neurol 2009;8:165–174.
19. Greenberg SM, Eng JA, Ning M, Smith EE, Rosand J. Hemorrhage burden predicts recurrent intracerebral hemorrhage after lobar hemorrhage. Stroke 2004;35:1415–1420.
20. Greenberg SM, Rosand J. Outcome markers for clinical trials in cerebral amyloid angiopathy. Amyloid 2001; 8(suppl 1):56–60.
21. Rosand J, Muzikansky A, Kumar A, et al. Spatial clustering of hemorrhages in probable cerebral amyloid angiopathy. Ann Neurol 2005;58:459–462.
22. Vinters HV. Cerebral amyloid angiopathy: a critical review. Stroke 1987;18:311–324.
23. Pfeifer M, Boncristiano S, Bondolfi L, et al. Cerebral hemorrhage after passive anti-Abeta immunotherapy. Science 2002;298:1379.
24. Salloway S, Sperling R, Gilman S, et al. A phase 2 multiple ascending dose trial of bapineuzumab in mild to moderate Alzheimer disease. Neurology 2009;73:2061–2070.
25. Eckman MH, Wong LK, Soo YO, et al. Patient-specific decision-making for warfarin therapy in nonvalvular atrial fibrillation: how will screening with genetics and imaging help? Stroke 2008;39:3308–3315.

Editor's Note to Authors and Readers: Levels of Evidence coming to *Neurology*®

Effective January 15, 2009, authors submitting Articles or Clinical/Scientific Notes to *Neurology*® that report on clinical therapeutic studies must state the study type, the primary research question(s), and the classification of level of evidence assigned to each question based on the classification scheme requirements shown below (left). While the authors will initially assign a level of evidence, the final level will be adjudicated by an independent team prior to publication. Ultimately, these levels can be translated into classes of recommendations for clinical care, as shown below (right). For more information, please access the articles and the editorial on the use of classification of levels of evidence published in *Neurology*.[1-3]

REFERENCES

1. French J, Gronseth G. Lost in a jungle of evidence: we need a compass. Neurology 2008;71:1634–1638.
2. Gronseth G, French J. Practice parameters and technology assessments: what they are, what they are not, and why you should care. Neurology 2008;71:1639–1643.
3. Gross RA, Johnston KC. Levels of evidence: taking *Neurology*® to the next level. Neurology 2009;72:8–10.

Classification scheme requirements for therapeutic questions

Class I. A randomized, controlled clinical trial of the intervention of interest with masked or objective outcome assessment, in a representative population. Relevant baseline characteristics are presented and substantially equivalent among treatment groups or there is appropriate statistical adjustment for differences.

Class II. A randomized, controlled clinical trial of the intervention of interest in a representative population with masked or objective outcome assessment that lacks one criterion a-e in Class I or a prospective matched cohort study with masked or objective outcome assessment in a representative population that meets b-e in Class I. Relevant baseline characteristics are presented and substantially equivalent among treatment groups or there is appropriate statistical adjustment for differences.

Class III. All other controlled trials (including well-defined natural history controls or patients serving as their own controls) in a representative population where outcome is independently assessed or independently derived by objective outcome measurements.

Class IV. Studies not meeting Class I, II, or III criteria including consensus or expert opinion.

AAN classification of recommendations

A = Established as effective, ineffective, or harmful (or established as useful/predictive or not useful/predictive) for the given condition in the specific population. (Level A rating requires at least two consistent Class I studies.)

B = Probably effective, ineffective, or harmful (or probably useful/predictive or not useful/predictive) for the given condition in the specific population. (Level B rating requires at least one Class I study or two consistent Class II studies.)

C = Possibly effective, ineffective, or harmful (or possibly useful/predictive or not useful/predictive) for the given condition in the specific population. (Level C rating requires at least one Class II study or two consistent Class III studies.)

U = Data inadequate or conflicting; given current knowledge, treatment (test, predictor) is unproven.